

ERL: Energy Recovery Linacs

Chaivat Tengsirivattana

CASA, Jefferson Lab
University of Virginia

USPAS 2008: RF Superconductivity

Annapolis, MD

June 27, 2008

High-Current Energy-Recovering Electron Linacs

1. Introduction
2. Historical Development of Energy-Recovering Linacs
3. The Jefferson Laboratory Infrared Demonstration Free-Electron Laser
4. Overview of Energy-Recovering Linac Projects and Proposals
5. Scaling of Energy-Recovering Linacs to Higher Energies
6. Scaling of Energy-Recovering Linacs to Higher Currents

1.1 Traditional Types of Electron Accelerators

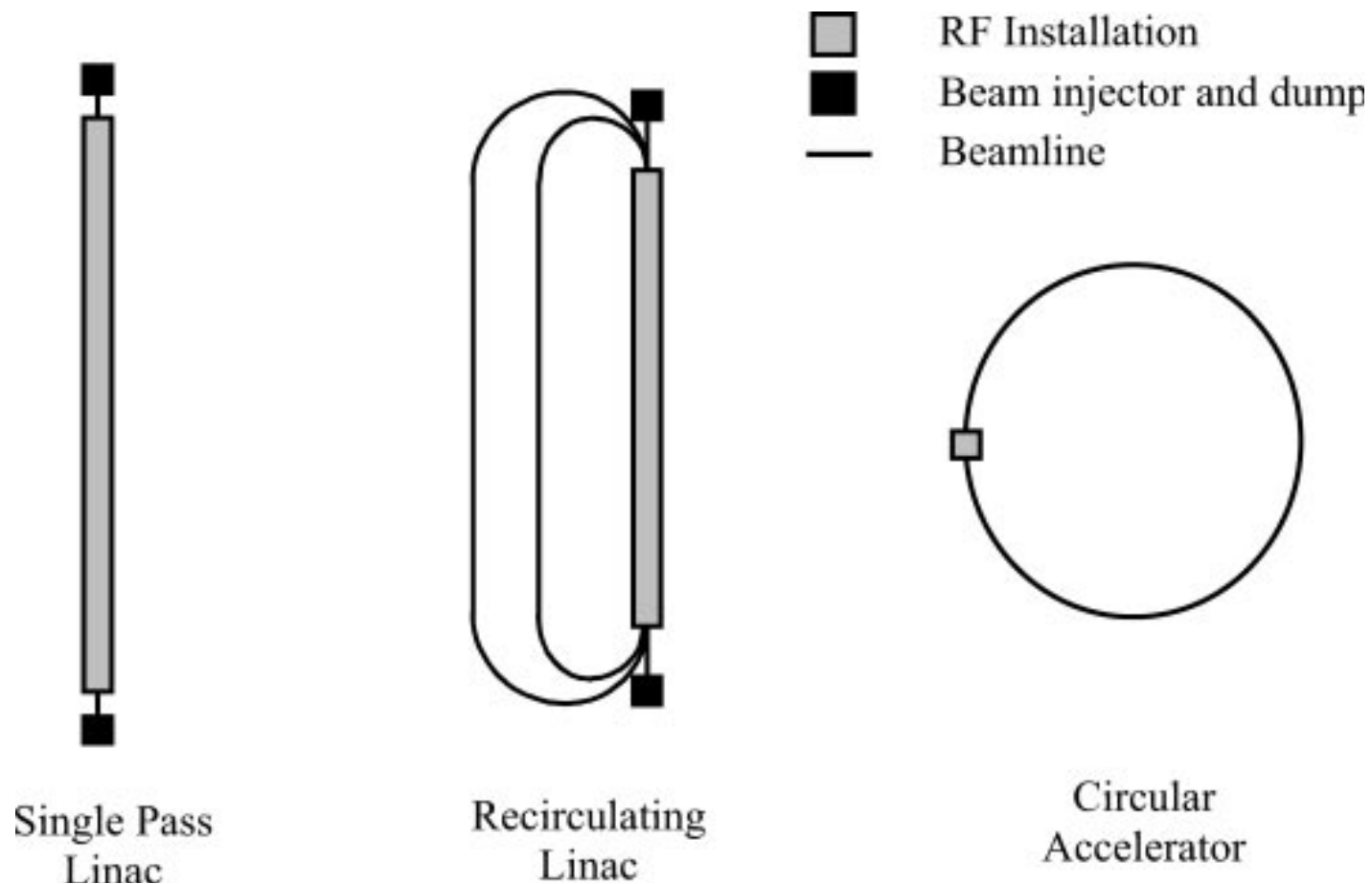


Figure 1 Main accelerator types.

1.2 Beam Recirculation

Multipasses

Accelerate - Decelerate

Linacs

1. Electron resides briefly.
2. Laser-driven photocathode – Polarization and control
3. Emittance
4. Pulse duration

Ring

1. Equilibrium – by radiation damping
2. Naturally bunched

1.3 Beam Energy Recovery

Simplest case: single recirculation

1. Accelerate in 1st pass
2. Recirculate in 2nd pass, plus ½ Rf wavelengths.

Efficiency: Rf to beam multiplication factor

$$\kappa = \frac{P_{beam}}{P_{RF}} \simeq \frac{I_b E_f}{I_b E_{inj} + P_{rf, linac}}$$

Accelerating gradients 20 MV/m

Quality factor 10^{10}

Continuous wave

2. Radiofrequency Superconductivity and Recirculating Linacs

Superconducting cavities:

1. CW or high-duty-factor
2. Highly efficient coupling
3. High-average-current
4. Reduction in length of the accelerator

3. Jefferson Laboratory Infrared Demonstration Free-Electron Laser

SRF CEBAF

- High-repetition-rate cw electron beam.
- High-brightness DC electron sources

3.1 JLab IR Demo FEL System Design

10 MeV to 35-48 MeV

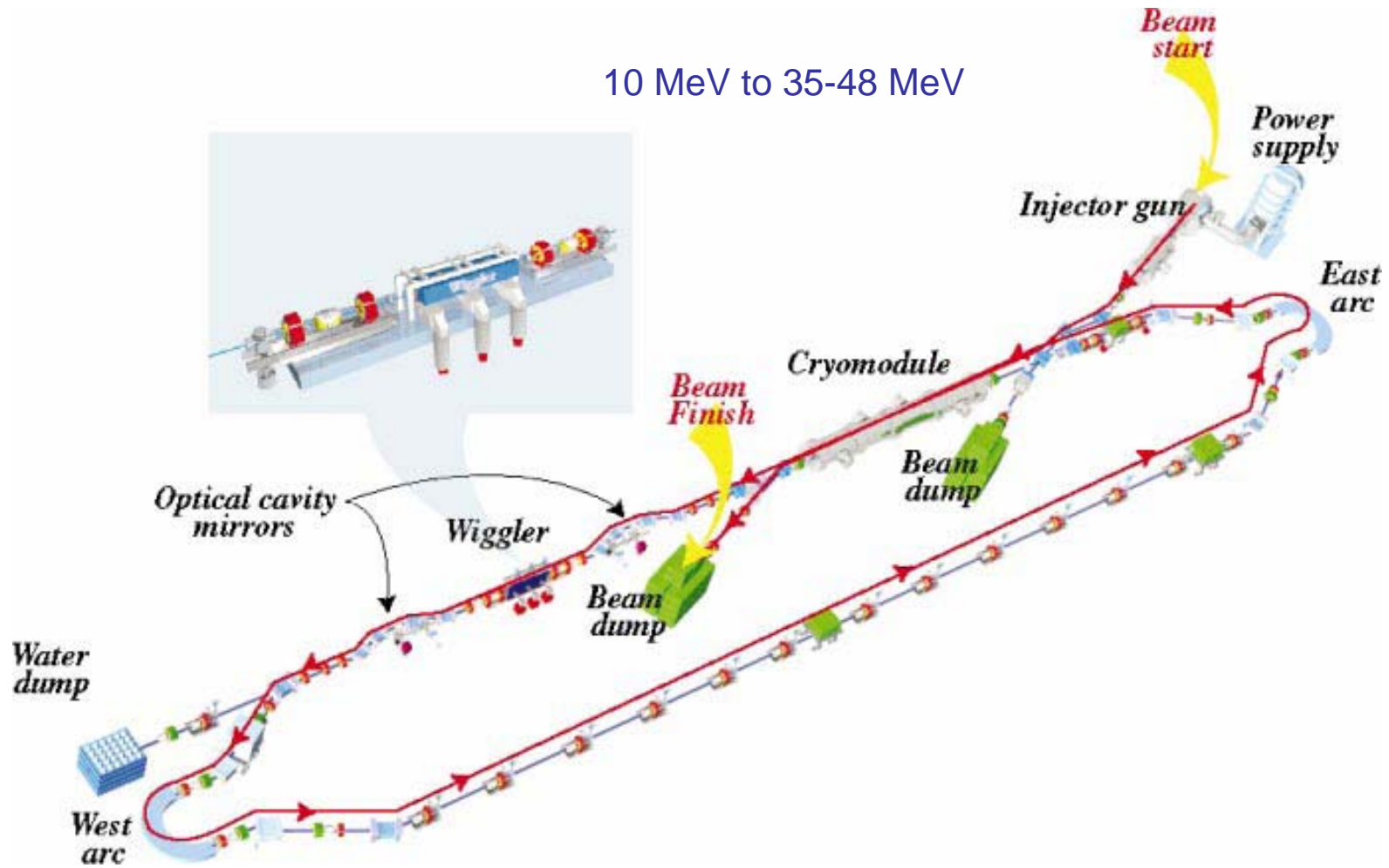


Figure 2 The Jefferson Laboratory Infrared Demonstration Free-Electron Laser.

Table 1 System parameters of the JLab IR Demo FEL

Parameter	Nominal	Achieved
Beam energy at wiggler	42 MeV	42 MeV
Average beam current	5 mA	5 mA
Bunch charge	60 pC	60–135 pC
Bunch repetition rate	74.85 MHz	18.7–74.85 MHz
Normalized emittance (rms)	13 mm-mrad	5–10 mm-mrad
Bunch length at wiggler (rms)	400 fs	400 fs
Peak current	60 A	60 A
FEL extraction efficiency	>0.5%	>1%
$\delta p/p$ before wiggler (rms)	0.5%	<0.25%
$\delta p/p$ after wiggler (full)	5%	6%–8%
cw FEL power	1 kW	2.13 kW

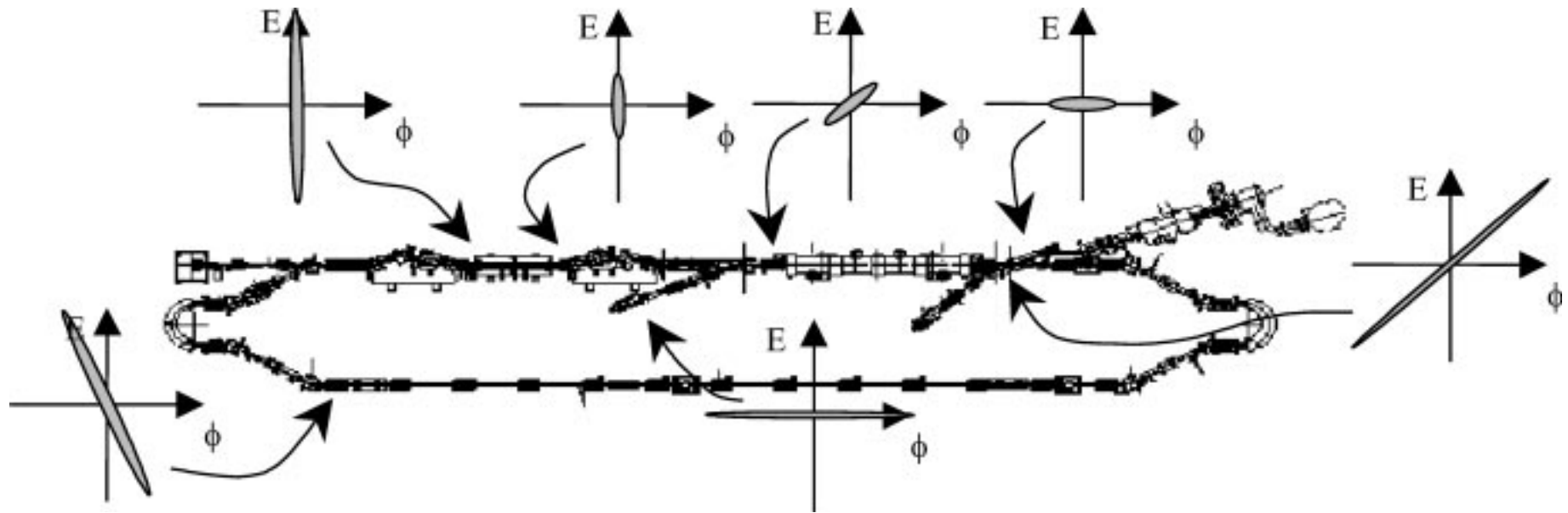


Figure 3 Longitudinal matching scenario in the JLab IR Demo FEL, showing phase versus energy diagrams at critical locations.

3.2 Longitudinal Matching

- 2-MeV full energy spread, 20% of 10 MeV.
- Energy recovery proved quite efficient.

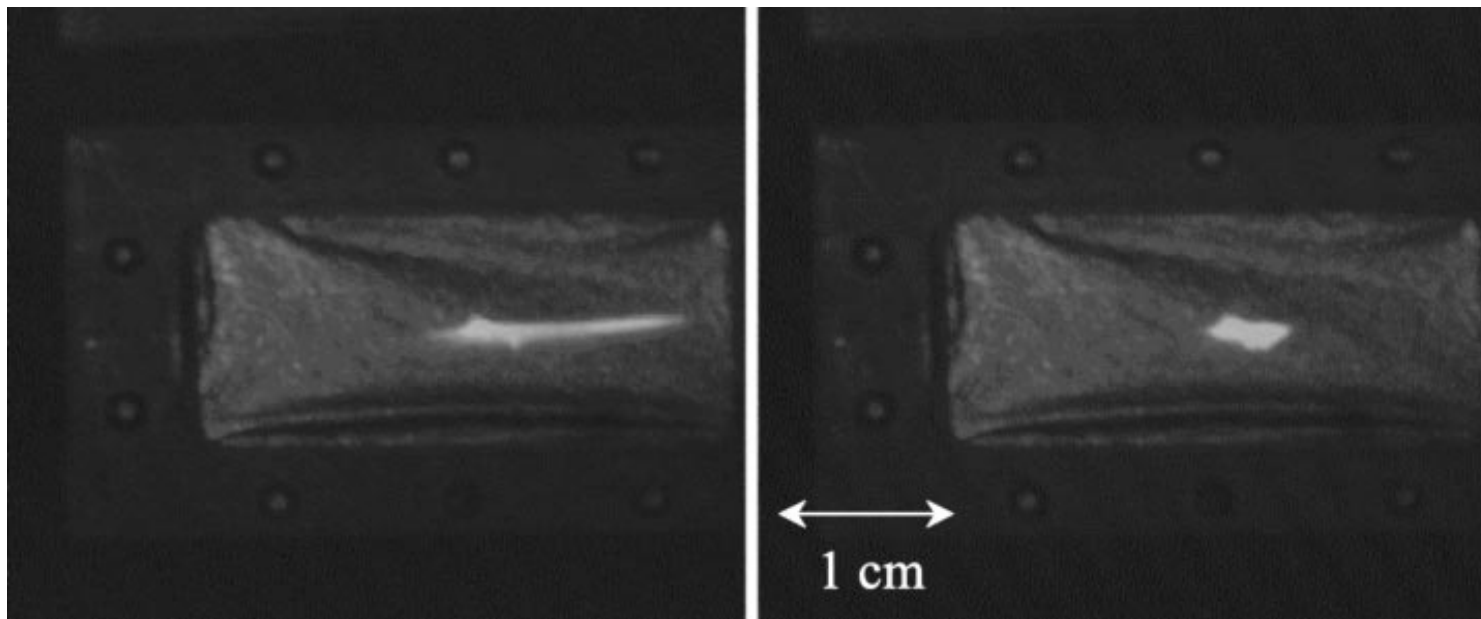


Figure 4 Beam viewer image in chicane downstream of FEL (dispersion of 0.4 m). Left: lasing, right: no lasing.

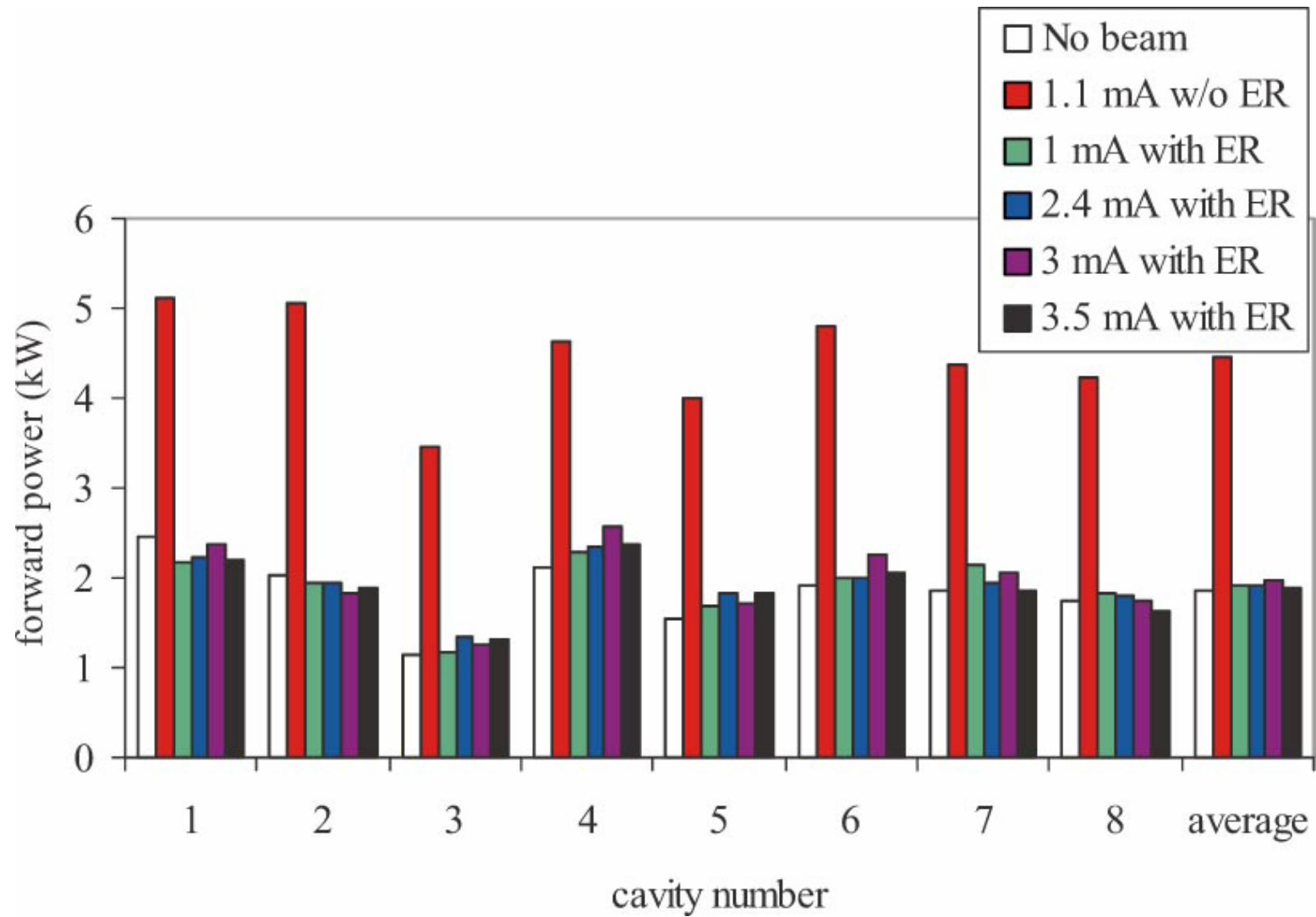


Figure 5 RF system generator power for each linac cavity without beam, without and with energy recovery at various current levels.

3.3 System Operation and Performance

Table 2 Chronology of the JLab IR Demo FEL

Date	Milestone
October 1997	first electron beam in vault (injector)
December 1997	first electron beam to straight-ahead dump
March 1998	high-current single-pass linac operation (1.1 mA cw to straight-ahead dump)
June 1998	wiggler installed, first light (155 W cw at 5 μm /1.1 mA straight ahead)
July 1998	recirculator construction completed, first energy-recovered beam, first (low-power) lasing with energy recovery
December 1998	high-power lasing with energy recovery (>200 W cw at 5 μm /1.4 mA)
March 1999	kW-class 5 μm operation (710 W cw at 3.6 mA, mirror limited)
July 1999	1.72 kW cw at 3 μm /4.4 mA; kW-class tunable light at 3, 5 and 6 μm 5th harmonic (1 μm) lasing
September 1999	detection of Thomson scattered x-rays
August 2001	2 kW IR operation
November 2001	final beam operations, including production of nearly 20 W THz radiation; decommissioning and start of 10-kW upgrade installation

3.4 10kW IR/1kw UV Upgrade

1. Doubling current, from 5 to 10 mA, bunch charge from 60 to 135 pC.
2. Installing 2 additional cryomodules, E - 160 MeV.
3. Upgrading the recirculators.
4. Adding a pair of optical cavities.

October 30th, 2006:

14.2kW at 9.1 mA and 150 MeV

160 MeV, 9.1 mA, 150 pC, 74.85 MHz, 7 mm-mrad, 150 fs

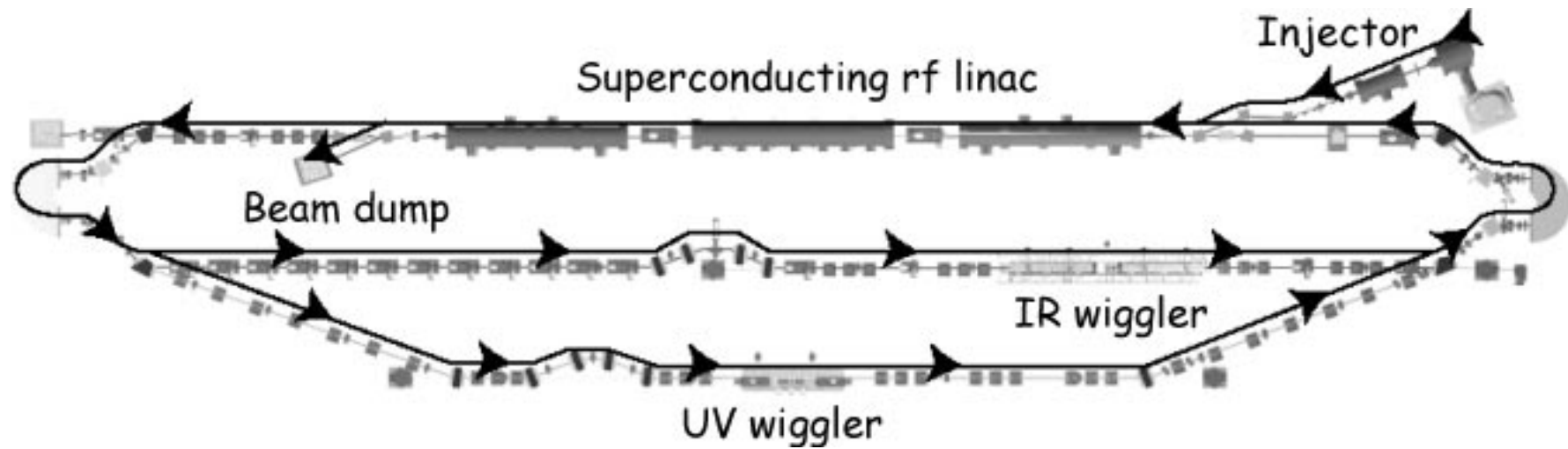


Figure 6 Schematic of JLab 10-kW IR/1-kW UV FEL upgrade configuration.

Table 3 System parameters of the JLab IR and UV FEL upgrade

Parameter	IR FEL Upgrade	UV FEL
Beam energy at wiggler	80–210 MeV	200 MeV
Average beam current	10 mA	5 mA
Bunch charge	135 pC	135 pC
Bunch repetition rate	74.85 MHz	74.85 MHz
Normalized emittance (rms)	13 mm-mrad	5–10 mm-mrad
Bunch length at wiggler (rms)	200 fs	200 fs
Peak current	270 A	270 A
FEL extraction efficiency	1%	0.25%
$\delta p/p$ before wiggler (rms)	0.5%	0.125%
$\delta p/p$ after wiggler (full)	10%	5%
CW FEL power	>10 kW	>1 kW

4.1 High-Average-Power FELs

- JAERI FEL, Japan
- Accelerator-Recuperator FEL, Novosibirsk, Russia
- KAERI FEL, Korea
- JLab 10-kW IR FEL Upgrade

4.2 ERL-Based Light Sources

ERLs:

- Average current-carrying capability of storage-ring.
- Smaller beam emittance and energy spread.
- Higher photon brilliance and coherence, round sources, and short-pulse-length radiation. 100-fsec pulse width domain.

- ERL at Cornell, 77pC, 1.3 GHz, 100 mA.
- PERL at Brookhaven.
- 4GLSP at Daresbury, UK.
- LUX at LBNL.

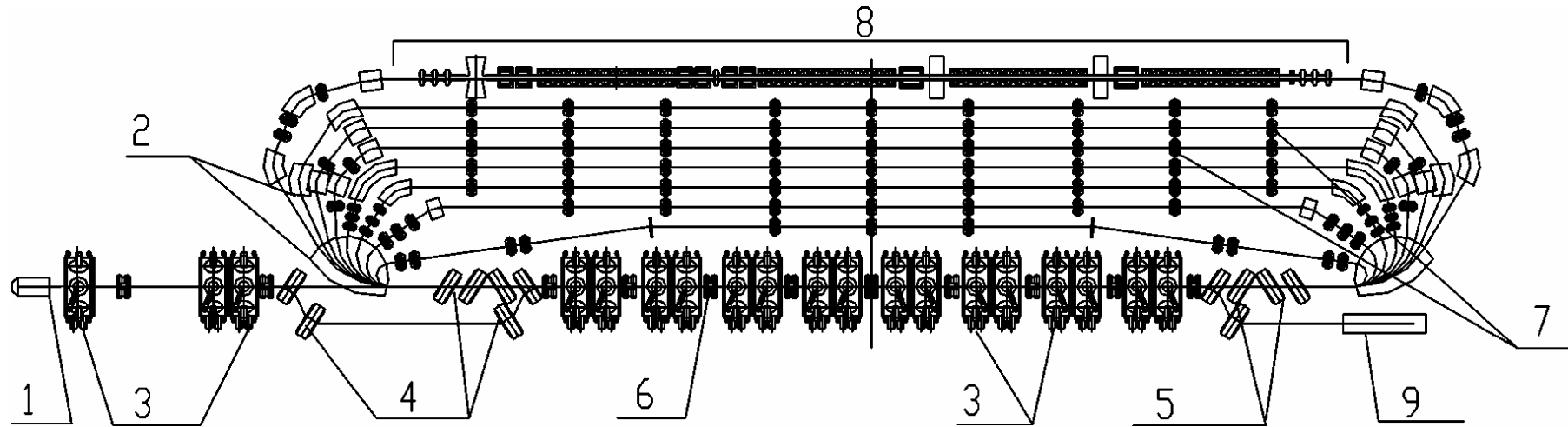


Figure 7 Accelerator-recuperator FEL in Novosibirsk. 1: electron gun; 2: bending magnets; 3: RF resonators; 4,5: injection and extraction magnets; 6: focusing quadrupoles; 7: straight sections with the quadrupole lenses; 8: FEL magnetic system; 9: beam dump.

4.3 Beam Electron Cooling

- Same gamma, act as heat sink – higher luminosity.

RHIC cooler – 50 MeV, 100 mA ERL.

- High-average-current source, but low frequency = 9 MHz, so high bunch charge = 10 nC.
- Maximize the longitudinal overlap to maximize the cooling rate, beam need to be debunched and rebunched.

4.4 Electron-Ion Colliders

- Advantageous and produce higher luminosity.
 - Ring: one damping time – 1,000 revolutions.
 - Increase N_i
 - eRHIC, ELIC
1. Cornell/JLab ERL phase I – 100 MeV, 100 mA.
 2. Brookhaven e-cooling prototype.
 3. JLab 10-kW FEL Upgrade.
 4. CEBAF-ER.

$$L = \frac{fN_e N_i}{2\pi \left(\sigma_{ex}^2 + \sigma_{ix}^2 \right)^{1/2} \left(\sigma_{ey}^2 + \sigma_{iy}^2 \right)^{1/2}}$$

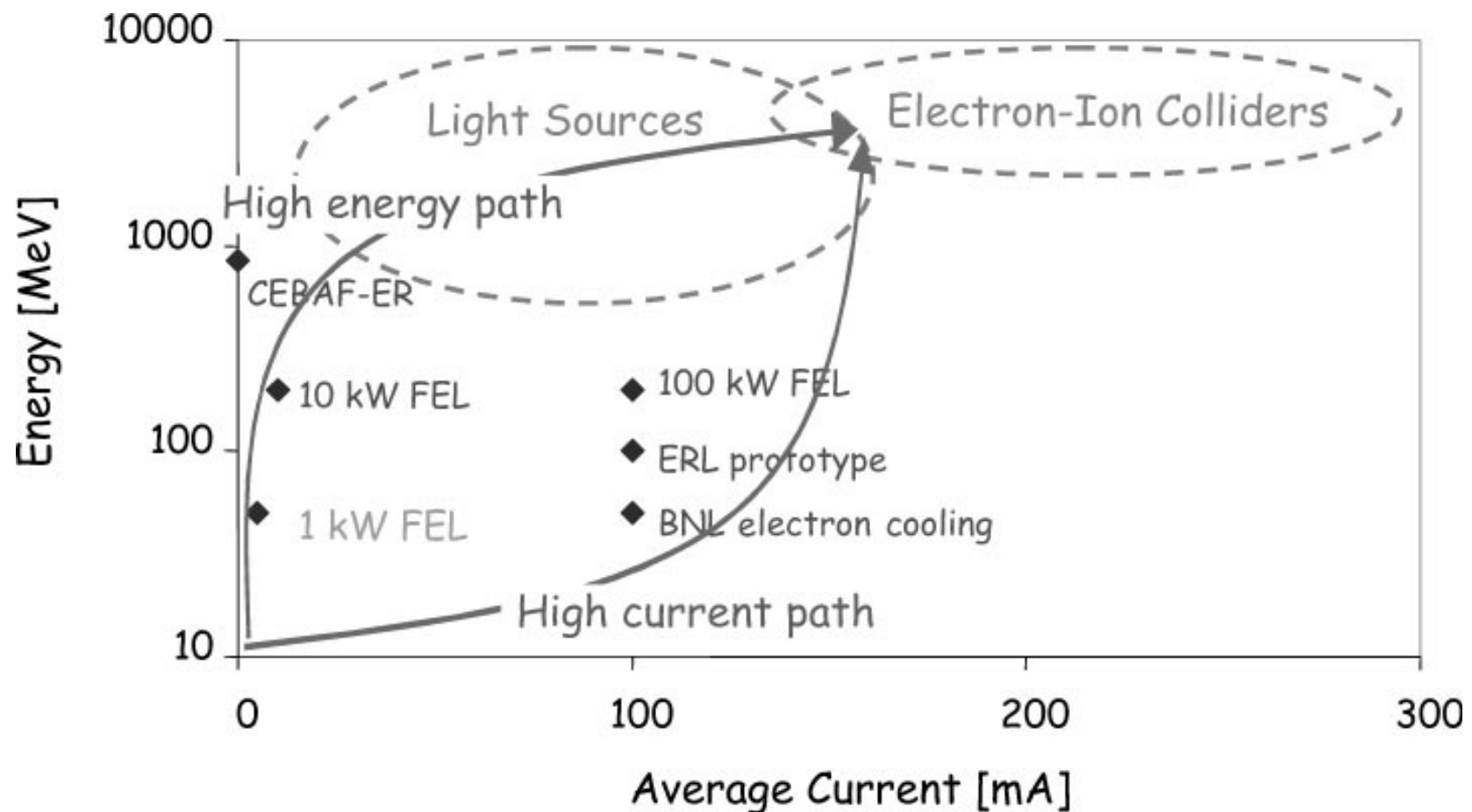


Figure 8 Energy-recovering linacs in terms of energy versus average current: existing, planned, and proposed ERL-based schemes.

5.1 Injection Energy

- Low E_i vs high E_i .

5.2 Number of Passes

- Cost-control measure and optimizing performance.

5.3 General Features of Machine Topology

- Use of spreaders and recombiners

5.4 Phase-Space Matching

- Longitudinal phase-space
- Transverse phase-space
- Graded-gradient focusing

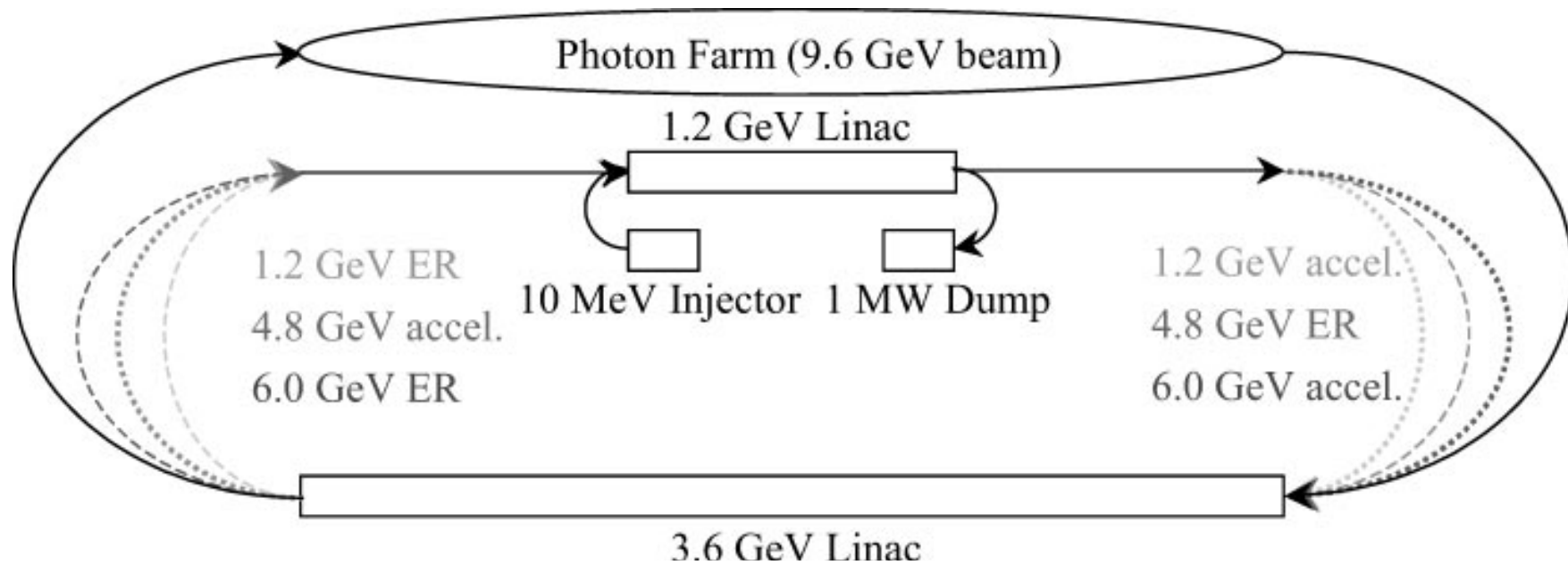


Figure 9 A split-linac topology for ERL-based light source.

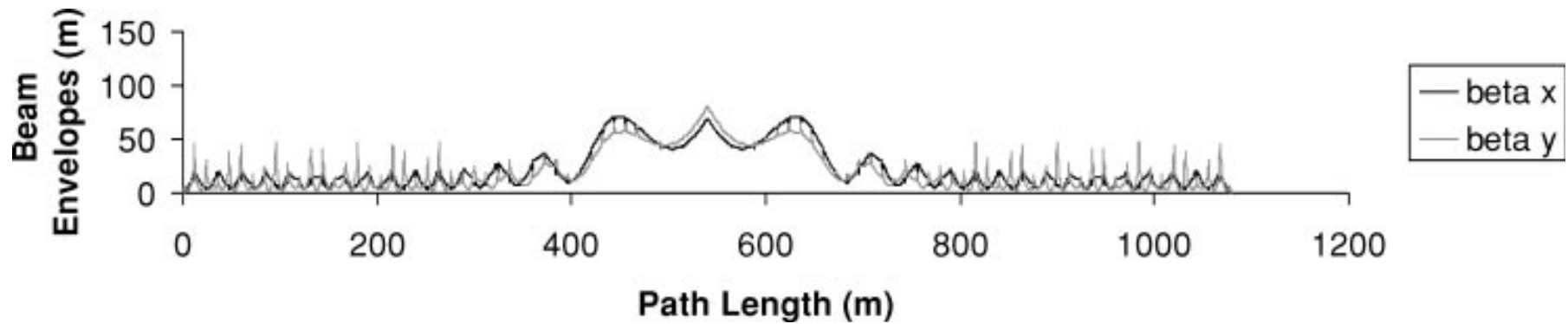


Figure 10 Beam envelopes (m) in a 10-MeV to 10-GeV recirculating, energy-recovering accelerator using graded-gradient focusing.

5.5 Phase-Space Preservation

- Transfer matrix element
- One parameter, one knob

5.6 Beam Halo

- Beam loss 0.1 μA out of 5 mA – kilowatts of lost beam power

5.7 CEBAF-ER Experiment

- Chicane – a half-rf-wavelength phase delay.
 1. Allow investigation of beam-quality preservation.
 2. Allow investigation of dynamic range (injected to full energy ratio).
 3. Large-scale demonstration.
- 1 GeV full energy and recovered it, 56 MeV injection Energy, cw and 80 μA .

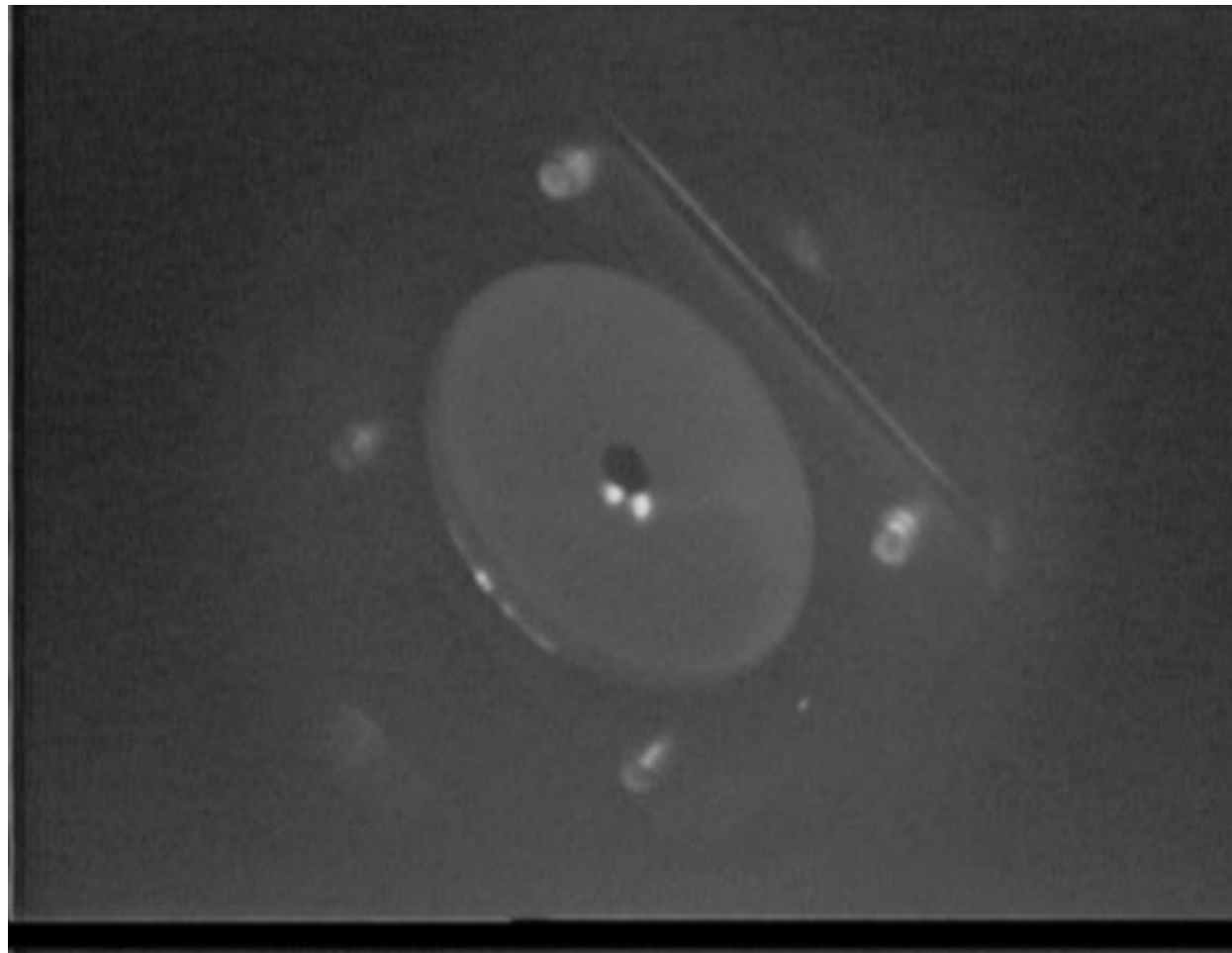


Figure 11 CEBAF-ER experiment. Accelerated (left) and recovered (right) beams at midpoint of the south linac. This viewer image demonstrates that the decelerating beam remained well-defined and of similar quality to the accelerating beam.

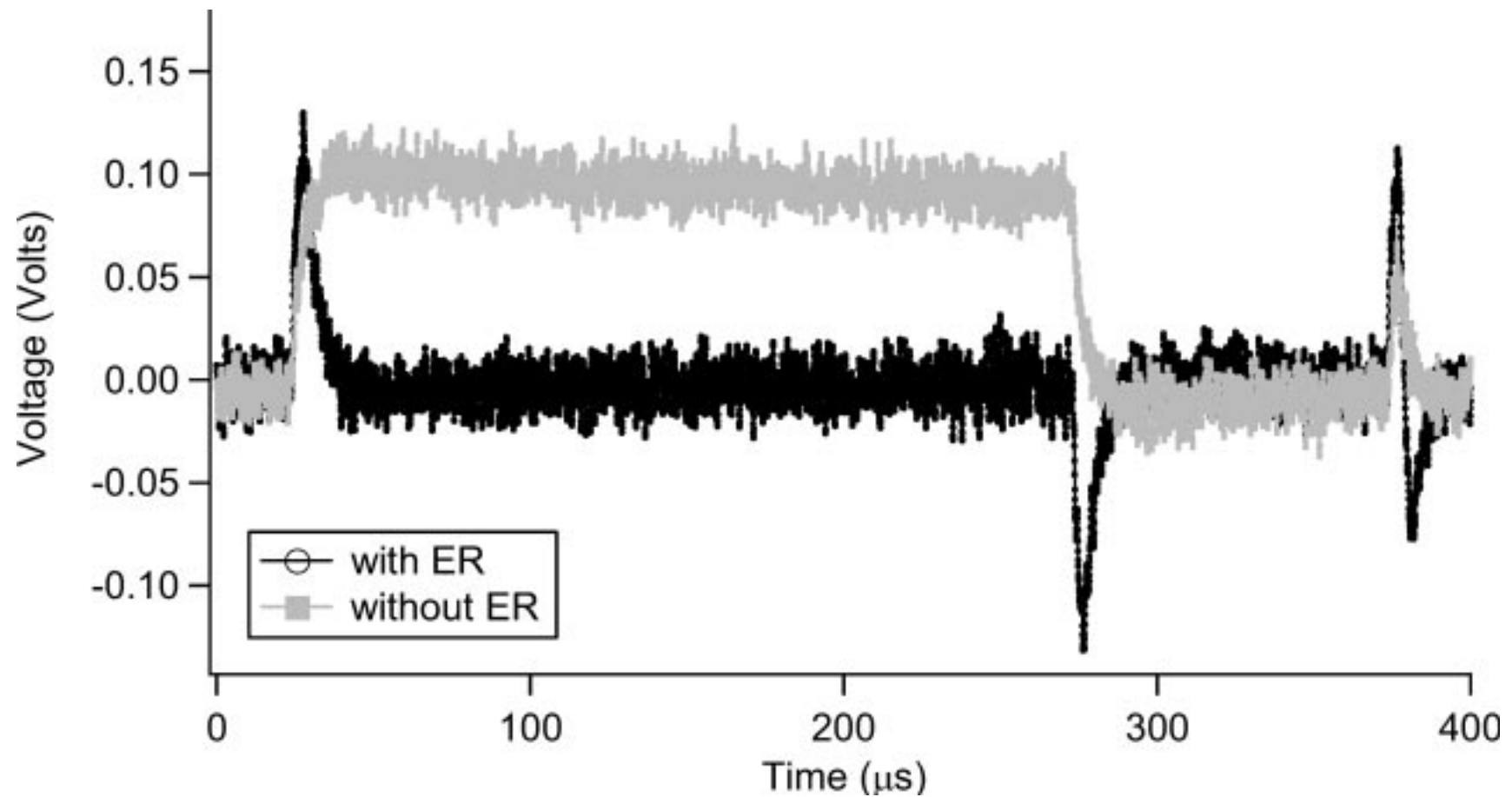


Figure 12 CEBAF-ER experiment. RF system gradient modulator drive signals during pulsed beam operation, with and without energy recovery.

6.1 Generation and Preservation of Low-Emittance, High-Current Beams

- Low emittance – 1 mm-mrad.
- Short bunch-length – 1 psec.
- Preservation in low energy regime – space charge effect.
- Linac and beam lines – wakefield effects.
- Recirculators – Coherent Synchrotron Radiation.

6.2 Multibunch Instabilities

- ERLs more susceptible, support current approaching or exceeding these threshold.
- Beam Breakups, HOMs

$$I_{th} = \frac{-2p_r c}{e(R/Q)_m Q_m k_m M_{ij} \sin(\omega_m t_r + l \pi/2) e}$$

Longitudinal BBU

- $i, j = 5, 6$ and m – longitudinal HOM.

Transverse BBU

- $i, j = 1, 2$ or $3, 4$ and m – transverse HOM.

Beam-loading instabilities

- $i, j = 5, 6$ and m – fundamental accelerating.

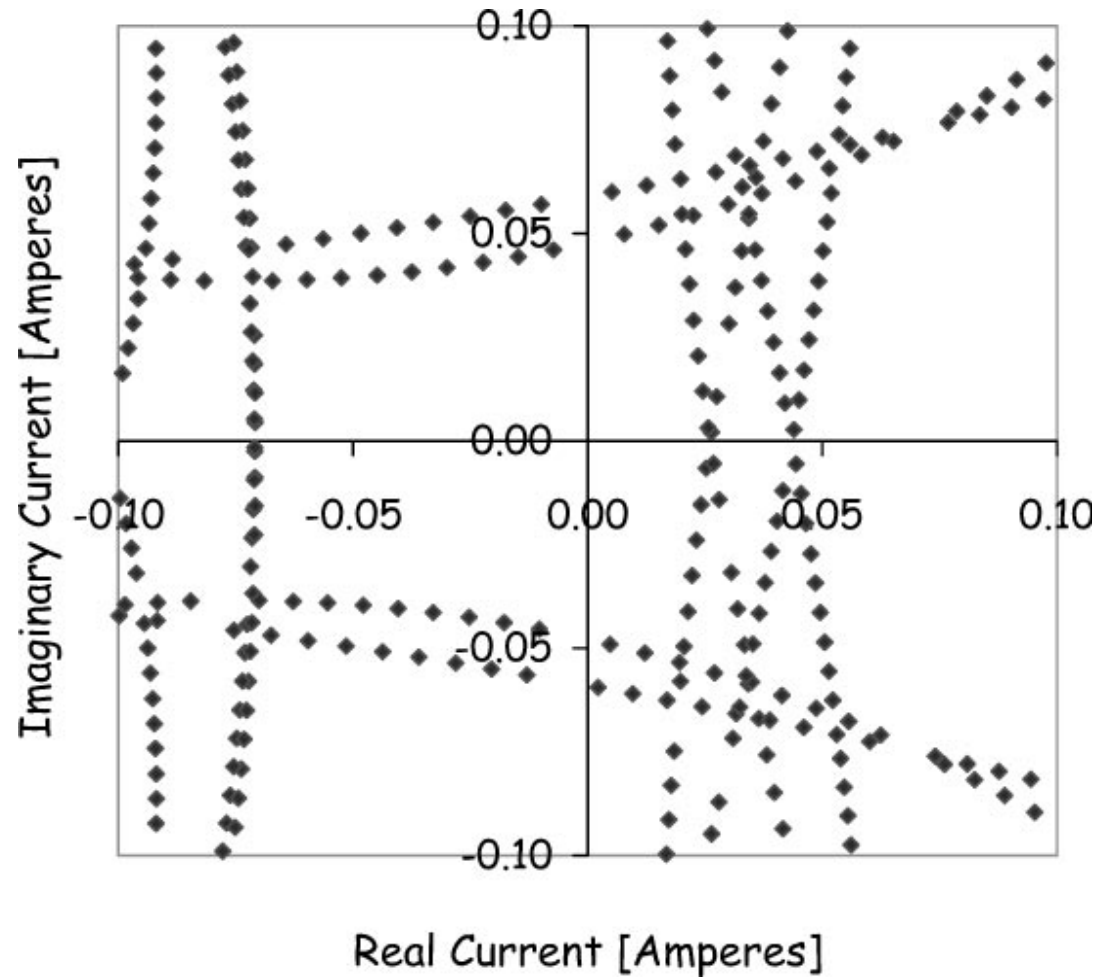


Figure 13 Beam breakup stability plot for the JLab IR Demo FEL,
By MATBBU codes.

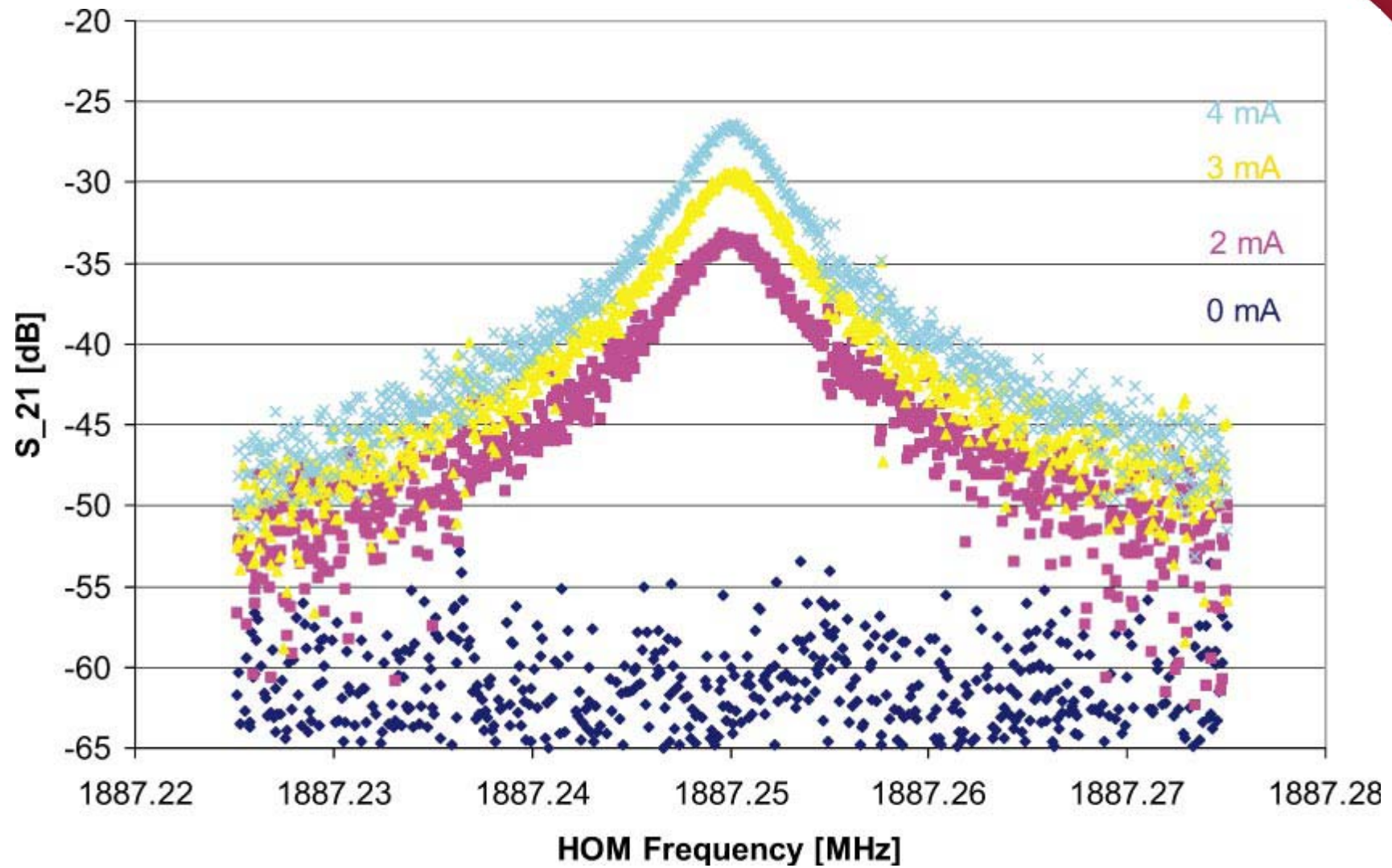


Figure 14 RF cavity response to beam excitation at higher-order mode frequency of 1887 MHz at various beam currents from 0 to 4 mA.

6.3 Superconducting RF Issues and HOM Power Dissipation

- cw beam – high average current.
- Multi GeV.
- Gradient – 20 MV/m
- $Q_0 - 1 \times 10^{10}$

- Extraction of HOMs
- Could be up to 1 kW per cavity, destroy cooper pairs

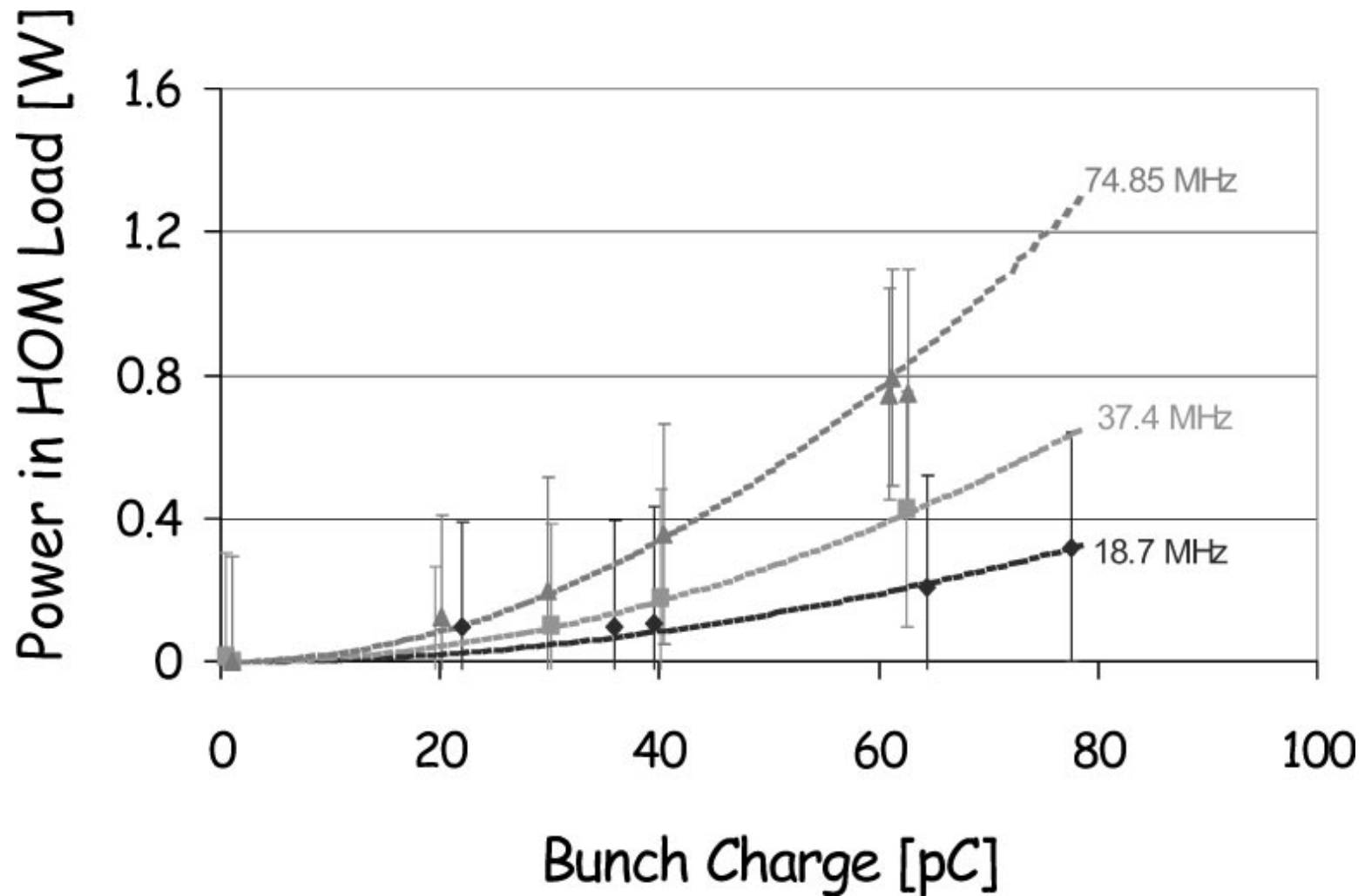


Figure 15 Measured higher-order mode (HOM) power dissipated in one of two HOM loads per linac cavity versus bunch charge at three bunch repetition rates.

6.4 RF Coupling Optimization and RF Control

- Multiplication factor increases as a function of the loaded quality factor Q_L .
- Microphonic vibrations.
- Radiation pressure during turn-on.
- Self-excited loop, Generator-driven system, or Hybrid.
- Piezo to suppress microphonic noise and Lorentz-force-detuning.